Contrast-Enhanced Ultrasonography–Based Hepatic Perfusion for Early Prediction of Prognosis in Acute Liver Failure

Hidekatsu Kuroda (iD) , Tamami Abe, Yudai Fujiwara, Tomoaki Nagasawa, Yuji Suzuki (iD) , Keisuke Kakisaka (iD) , and Yasuhiro Takikawa (iD)

BACKGROUND AND AIMS: Acute liver failure (ALF) is a rare but dramatic clinical syndrome characterized by massive hepatic necrosis leading to multiorgan failure. It is difficult to predict the outcomes in patients with ALF using existing prognostic models. We aimed to analyze hepatic perfusion using contrast-enhanced ultrasound and Doppler ultrasound in patients with ALF and investigate its utility as a prognostic biomarker.

APPROACH AND RESULTS: In this prospective observational study, 208 patients with acute liver injury/ALF were enrolled from 2015 to 2019. We evaluated 50 consecutive patients with ALF with Doppler ultrasound and contrast-enhanced ultrasound performed on admission. The cases were divided into the following two groups: survivors (recovered without surgical intervention) and nonsurvivors (died of ALF or underwent liver transplantation). The time to peak and peak intensity of hepatic artery, portal vein, hepatic vein, and liver parenchyma were calculated using the time-intensity curve analysis. The hepatic artery (HA) resistive index was calculated using the fast Fourier transform analysis of Doppler ultrasound. The time interval (TI) between the time to peak of HA and liver parenchyma (LP) was significantly shorter in the nonsurvivors than in the survivors ($P < 0.0001$). The area under the receiver operating curve values for TI (HA, LP), Japanese scoring system, HE prediction model, Model for End-Stage Liver Disease score, and King's College Hospital criteria for the prediction of poor prognosis were 0.953, 0.914, 0.861, 0.816, and 0.731, respectively. The most appropriate cutoff value of TI (HA, LP) was 6.897 seconds; the sensitivity, specificity, positive and negative predictive values were 94.4%, 90.6%, 85.0%, and 96.7%, respectively.

CONCLUSIONS: TI (HA, LP) accurately predicts the outcome in patients with ALF and may be useful in clinical decision making. (HEPATOLOGY 2021;73:2455-2467).

Acute liver failure (ALF) is a clinical syndrome with a variety of causes resulting in rapid loss of hepatocyte function. It is typically associated with coagulopathy and encephalopathy and causes significant morbidity and mortality.[1,2] The clinical treatment of ALF involves intensive therapy including artificial liver support consisting of plasma exchange and continuous hemodiafiltration; however, the morbidity and mortality remain high.[3,4] In contrast, liver transplantation (LT) has been an innovative treatment option for ALF and has led to the reduction in the deaths of thousands of high-risk patients.[5-7] However, it is expensive, necessitates

life-long immunosuppression, and is limited by the global shortage of available organs.[8] It is known that the early prediction of the development of HE and early initiation of intensive therapy can improve the prognosis of patients with severe acute liver injury (ALI).[9] Thus, it is necessary to predict the outcome early in patients with ALF who are at risk of death if LT is not performed, as well as in patients who are expected to survive with intensive care. Therefore, there is an urgent need to develop early and noninvasive techniques that can predict massive hepatic necrosis resulting from ALF and also help in evaluating the need for LT. The severity of liver-tissue damage and the immediate reconstruction of liver tissue in ALF are critical factors that affect the prognosis.[10,11] Histological examination of liver biopsy specimens obtained through transvenous biopsies can be used to assess liver damage and reconstruction. However, liver biopsy can be dangerous and impractical in seriously ill patients; thus, clinicians are forced to rely on clinical findings.[12] In contrast, prognostic models like the Model for End-Stage Liver Disease (MELD) score, the King's College Hospital criteria (KCHC), the HE prediction model, and the Japanese scoring system (JSS), used to predict the mortality in patients with fulminant hepatitis and late-onset hepatic failure are useful for assessing the risk of poor outcome in patients with ALF.[9,13-15] However, MELD and its variations have been criticized for including laboratory measurements in the model, which vary from one laboratory to another, and therefore are difficult to standardize and replicate worldwide.[16]

Hepatic perfusion is a major determining factor in hepatic repair and the regenerative capability.[17,18] Previous studies using multidetector CT in patients with ALF have shown abnormal hepatic perfusion.[19-21] Tanaka et al. showed that increased hepatic arterial blood flow during the acute phase may act as a marker for the early recovery from hepatitis-induced damage.[22] Contrast-enhanced ultrasound (CEUS) perfusion imaging permits tissue hemodynamic imaging and is advantageous, as it is noninvasive and can be performed at the bedside of a seriously ill patient.[23] Miyazaki et al. showed that CEUS is a useful method to estimate the changes in hepatic hemodynamics in patients with ALI.[24] CEUS-derived time-intensity curves (TICs) reflect the hemodynamics of the tissue of interest by measuring the changes in the intensity of the harmonic frequencies versus time.[25,26] As a result, CEUS with TIC analysis enables the quantitative evaluation of the hepatic perfusion. However, so far, no studies have been designed to assess the usefulness of CEUS in estimating liver tissue damage, such as massive necrosis, and for the early prediction of the prognosis in patients with ALF.

Therefore, the primary goal of our prospective study was to measure hepatic perfusion using CEUS with TIC analysis in patients with ALF and to investigate the usefulness of CEUS for the early prediction of the prognosis in patients with ALF.

Materials and Methods

PATIENTS

This prospective observational study enrolled 208 patients with ALI and ALF between October 2015 and November 2019 (Fig. 1). The inclusion criteria for registration were as follows: no diagnosis of either chronic hepatitis or cirrhosis, ALI (aspartate aminotransferase > 200 IU/L and/or alanine aminotransferase > 300 IU/L) and prothrombin time (PT) to international normalized ratio (PT-INR) > 1.2, or PT activity < 80%. After registering, 53 patients met the criteria for ALF. ALF was defined as the presence of

ARTICLE INFORMATION:

From the Division of Hepatology, Department of Internal Medicine, Iwate Medical University, Yahaba-cho, Japan.

ADDRESS CORRESPONDENCE AND REPRINT REQUESTS TO:

Hidekatsu Kuroda, M.D., Ph.D.
Division of Hepatology, Department of Internal Medicine
Iwate Medical University
Nishitokuta 2-1-1

Yahaba-cho, Shiwa-gun, Iwate, 028-3694, Japan
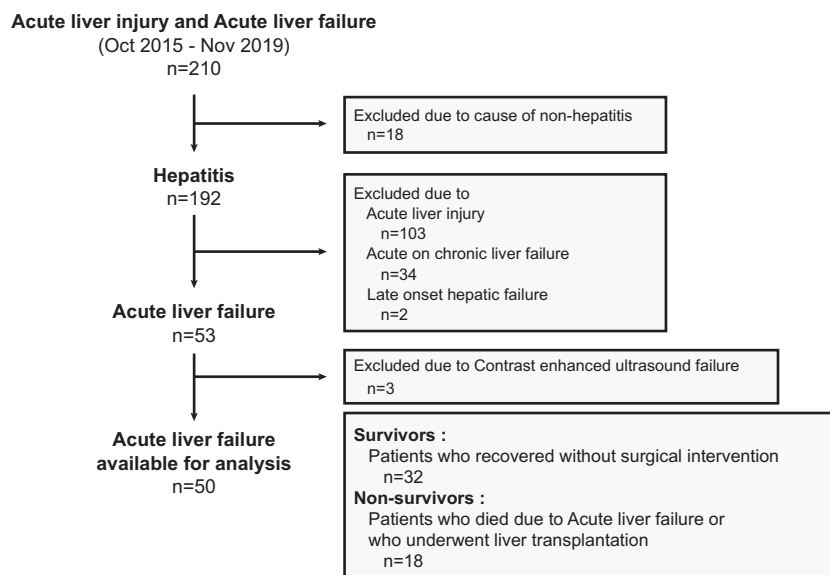E-mail: hikuro@iwate-med.ac.jp
Tel.: +81-19-651-5111

Acute liver injury and Acute liver failure
(Oct 2015 - Nov 2019)
n=210

Excluded due to cause of non-hepatitis
n=18

Hepatitis
n=192

Excluded due to
Acute liver injury
n=103
Acute on chronic liver failure
n=34
Late onset hepatic failure
n=2

Acute liver failure
n=53

Excluded due to Contrast enhanced ultrasound failure
n=3

Acute liver failure available for analysis
n=50

Survivors :
Patients who recovered without surgical intervention
n=32
Non-survivors :
Patients who died due to Acute liver failure or
who underwent liver transplantation
n=18

FIG. 1. Flow chart of eligible patients with ALF.

coagulopathy (PT-INR > 1.5 or PT activity < 40%) occurring within 8 weeks of the first onset of symptoms in patients without underlying liver disease.[27] All patients received intensive therapy including artificial liver support consisting of plasma exchange and/or continuous hemodiafiltration that were administered since the diagnosis of ALF with HE. LT was performed according to the JSS, to predict the prognosis of ALF.[14] Of the 53 patients with ALF enrolled in this prospective study aimed to assess the potential of CEUS findings as an early imaging biomarker for the prognosis in patients with ALF, 3 were excluded because their CEUS images could not be obtained due to the disturbance of consciousness in the patients related to hepatic coma.

All of the remaining patients (n = 50) were divided into "survivors" (n = 32) and "nonsurvivors" (n = 18) groups. The survivors were patients who recovered following intensive therapies including artificial liver support, whereas the nonsurvivors were patients who either died of ALF or underwent LT because there was no response to intensive therapies. The control group consisted of 10 subjects matched according to the mean age and sex ratio of the patients with ALF, and all had normal liver enzyme levels. All of the protocols followed in this study were approved by the institutional review board of Iwate Medical University (approval number H20-36). All of the patients provided written, informed consent before the study, in accordance with the principles of the Declaration of Helsinki (revision of Fortaleza, 2013).

CEUS IMAGING

CEUS was performed at baseline before the initiation of treatment, and after 7 days. Ultrasonography was performed using Aplio500 (Canon Medical Systems, Ohtawara, Japan) and 3.5-MHz convex transducer ultrasound probe. All ultrasound images were analyzed by two radiologists (H.K. and A.T. who have 20 years of experience in performing abdominal ultrasound examinations) who were blinded to the treatment information. CEUS imaging was recorded for 60 seconds immediately after the injection of a bolus (0.0075 mL/kg) of Sonazoid (perfluorobutane microbubbles; GE Healthcare, Oslo, Norway). The acoustic power of the contrast harmonic sonography was set to the default setting with a mechanical index of 0.25, a rate of 12 frames per second, dynamic range of 70 dB, gain of 70, depth of 11-13 cm, and focus of 8.0 cm, following the methods recommended by the guidelines.[28] In each patient, the right hepatic artery (HA), right portal vein (PV), hepatic vein (HV), and liver parenchyma (LP) were simultaneously scanned using the right intercostal view. Following the injection

of Sonazoid, the patients were asked to hold their breath for as long as possible (at least 20 seconds); the cine sequences were saved in a digital imaging and communication in medicine file format for subsequent analyses.

TIC ANALYSIS

The TIC analysis was performed using an offline personal computer with an image analysis software program (ImageJ; National Institutes of Health, Bethesda, MD). First, we decompressed the cine saved in Audio Video Interleave (AVI) format into uncompressed AVI files. In the uncompressed AVI file, the interval of each frame was 1/15th of a second. A total of 15 frames of the grayscale images were processed per second using the ImageJ software program. We observed the cine image frame by frame and set the time of the first echogenic microbubble observed in the HA at baseline. A circular region of interest (ROI) was established within the HA, PV, HV, and LP, and the intensity values were measured automatically using the ImageJ software program. The ROI with a 5-mm diameter was set on the HV 3-5 cm from the inferior vena cava and on the first branch of the HA or PV. Then, the ROI with a 10-mm diameter was set on the LP area, avoiding vessels, and at the same depth as the other ROIs (Fig. 2A). The intensity value of each pixel was expressed as 0 at minimum and 255 at maximum. After measuring the intensity values in the ROIs, we created a TIC of the arterial phase for 20 seconds from the time the contrast agent arrived at HA, using the Excel software program (Microsoft, Redmond, WA). The time to peak (TTP) and peak intensity (PI) were evaluated according to the TIC. We then calculated the time intervals (TIs) between TTP of HA and PV (TI [HA, PV]), HA and LP (TI [HA, LP]), and PV and LP (TI [PV, LP]). Furthermore, we calculated and recorded the arrival times of HA and HV, and then HA to HV transit time (HA-HVTT), with reference to previous reports[29] (Fig. 2B-F). All TIC parameters were measured until recovery or death, from hospital admission, at 7-day intervals. The investigators (H.K. and T.A.) were blinded to all patient data. All TIC parameters were measured three times for each patient, to investigate the intra-observer variability. Furthermore, the TI (HA, LP) of all patients was successively evaluated by two investigators to determine interobserver variability.

FAST FOURIER TRANSFORM ANALYSIS OF DOPPLER ULTRASOUND SIGNALS

We evaluated the peak systolic maximum velocity (Vmax) of the right HA, right PV, and HA resistive index (HARI) for the controls and all patients using the FFT analysis of Doppler ultrasound signals just before CEUS. The FFT analysis of the Doppler ultrasound signals was performed as described in previous reports, and the procedure is summarized as follows: The Aplio500 ultrasound scanner (Canon Medical Systems) was used with a 3.5-MHz convex transducer ultrasound probe. The ultrasound scanning was performed with the patient in the supine position. The Doppler ultrasonography was used initially for the detection of the right HA and right PV, and a Doppler waveform was obtained (Supporting Fig. S1A,B). The Vmax and the end-diastolic flow velocity (Vmin) were obtained after correcting for the angle of insonation, and then HARI ([Vmax–Vmin]/Vmax) was calculated.

PROGNOSTIC MODELS FOR ALF

In all patients, biochemical tests, CT imaging, and CEUS were performed on the first day at the hospital. The CT-derived liver volume (CTLV)/standardized liver volume (SLV) was calculated using the formula by Urata et al.[30] Liver atrophy was assessed by the CTLV/SLV ratio. In the present study, we performed a comprehensive evaluation to identify the independent prognostic factors from among the parameters recorded at admission, including results of biochemical tests, CTLV/SLV ratio, and the TIC parameter, using univariate and multivariate regression analysis.

The MELD score, KCHC, HE-prediction model, and JSS for ALF were calculated for each patient based on the results of the hematological examination and background information of the patient on admission. The early predictive performance of the TIC parameter, MELD score, KCHC, HE-prediction model, and JSS for ALF to predict the prognosis of ALF was assessed by receiver operating characteristic (ROC) analysis. The cutoff values for the prognostic prediction were estimated using the area under the ROC (AUROC).
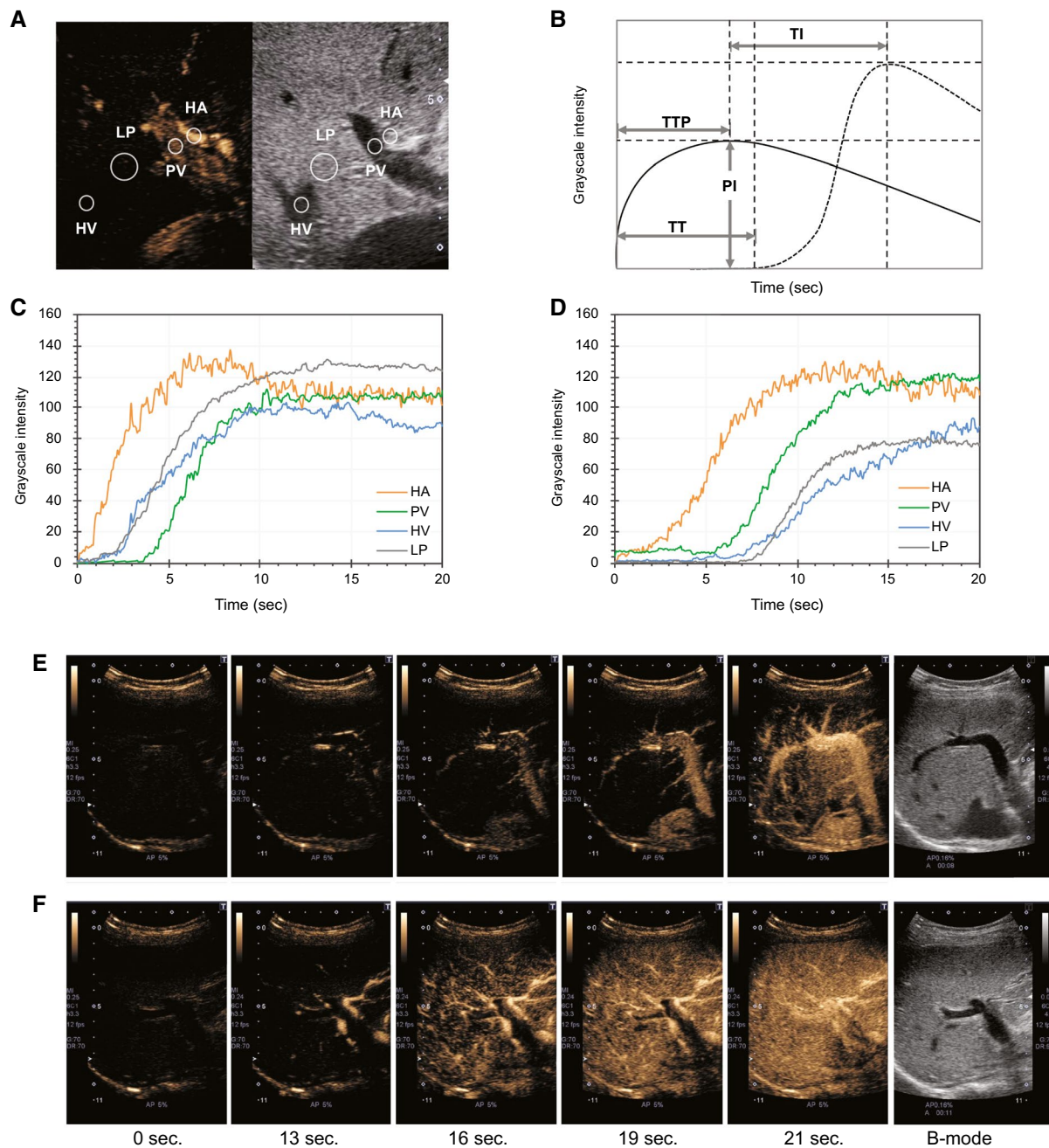
FIG. 2. Intensities of the HA, PV, HV, and LP were measured by setting circular ROIs using ImageJ software. (A) The ROIs were set at a depth of 6-8 cm (±3 cm from the focus point) from the surface. (B) Schematic TIC describing events after the bolus injection. The TTP indicates the duration from the first appearance of the contrast agent in the HA until maximum enhancement was reached. The PI indicates the maximum enhancement after subtracting the baseline intensity. The TI indicates the duration between two curves of TTP. The transit time (TT) describes the period of arrival time between two curves. TIC of the liver in a survivor (C) and nonsurvivor (D). The orange line is the signal intensity of the HA; the green line is the signal intensity of the PV; the blue line is the signal intensity of the HV; and the gray line is the signal intensity of the LP. In the nonsurvivor, the slope of the HA and LP are steeper, and the TTP is short compared with that observed in the survivor. CEUS perfusion imaging of the liver in a survivor (E) and a nonsurvivor (F). In the liver of the nonsurvivor, the HA and LP were enhanced steeply, whereas the PV was enhanced slowly.

STATISTICAL ANALYSIS

Statistical analyses were performed using the SPSS software program for Windows, version 23 (IBM, Armonk, NY). The values are presented as the mean ± SD or median (25th-75th percentiles) according to the distribution of the variables. A statistical analysis of the differences in TIC or FFT parameters among control, survivors, and nonsurvivors was performed using the Tukey–Kramer method. Interobserver and intra-observer agreement were evaluated using the intraclass correlation coefficient (ICC) for TI (HA, LP). Logistic regression analysis was used to determine the factors associated with nonsurvivors. ROC curves were constructed, and AUROC was calculated by the trapezoidal rule. Optimal cutoff values for the prediction of nonsurvivors were identified from the highest Youden index and were selected to maximize the sensitivity and specificity. The sensitivity, specificity, positive predictive value (PPV), and negative predictive value (NPV) were calculated using cutoffs obtained from the ROC curves. Repeated-measures ANOVA was used to assess changes in TI (HA, LP) over the course of 7 days. P values less than 0.05 were considered statistically significant.

Results

BASELINE CHARACTERISTICS OF THE PATIENTS

A total of 53 patients were enrolled in the study. The success rate for CEUS was 94.3% (50 of 53), since 3 patients were excluded due to their inability to perform the breath-holding procedure optimally. Therefore, 50 (94.3%) patients were included in the statistical analysis. The background characteristics of the 10 control subjects, the patients in the two groups, and their laboratory data on admission are summarized in Table 1. There were significant differences in the PT-INR, HGF, coma grade ≥ II (%), CTLV/SLV ratio, MELD score, KCHC (%), HE-prediction model, and JSS for ALF between the survivors and nonsurvivors. Pathological findings of the hepatic surgical specimen or autopsy tissue in nonsurvivors revealed massive or submassive hepatic necrosis in all of the cases (18 of 18: 100%).

TIC AND FFT PARAMETERS IN THE CONTROLS, SURVIVORS, AND NONSURVIVORS

Table 2 lists the comparison of the TIC and FFT parameters among the controls, survivors, and nonsurvivors. The nonsurvivors showed significantly shorter TTP (HA) (P = 0.035), TTP (LP) (P = 0.005), and TI (HA, LP) (P < 0.0001) than the survivors. PI (PV) and PI (LP) were significantly lower in the nonsurvivors than in the survivors (P = 0.012, P = 0.026). There were no statistically significant differences in the HA-HVTT and FFT parameters between the survivors and nonsurvivors. Each TI (HA, LP) was plotted into three categories: patients who recovered following intensive therapies including artificial liver support (n = 32), patients who received LT (n = 6), and patients who died (n = 12) (Fig. 3). The median TIs (HA, LP) in patients who survived, received LT, or died from liver failure were 8.31, 5.77, and 4.73 seconds, respectively. A significant difference was noted between survivors and LT patients, and between survivors and those who died. The ICC for intra-observer agreement on TI (HA, LP) measurements was 0.820 (95% CI: 0.745-0.882). Furthermore, the reproducibility of TI (HA, LP) between observers (for all patients) yielded an ICC of 0.791 (95% CI: 0.708-862).

PREDICTIVE FACTORS ASSOCIATED WITH NONSURVIVORS BY UNIVARIATE AND MULTIVARIATE REGRESSION MODELS

We analyzed the predictive factors associated with nonsurvivors from the baseline parameters at admission. Univariate regression analysis revealed that etiology (P = 0.045), PT-INR (P = 0.019), HGF (P = 0.005), coma grade ≥ II (P = 0.019), CTLV/SLV ratio (P = 0.014), and TI (HA, LP) (P = 0.002) were significant parameters for predicting poor prognosis. Furthermore, these factors were analyzed using multiple regression analysis, which revealed that TI (HA, LP) (P = 0.016) was the only independent factor for predicting poor prognosis (Table 3).

TABLE 1. Clinical Features and Laboratory Data of the Study Cohort on Admission

Characteristics	Control	Survivors	Nonsurvivors	Overall
No. of patients	10	32	18	50
Sex (male/female)	4/6	13/19	8/10	21/29
Mean age, years (range)	58.0 (28-65)	58.5 (20-79)	58.3 (27-76)	58.5 (20-79)
Etiology (n)				
HAV		1	1	2
HBV		9	4	13
Drug		6	3	9
AIH		8	4	12
Unknown		8	6	12
T.Bil (mg/dL)	0.7 (0.5-0.9)	9.3 (4.4-15.4)*	11.3 (7.4-20.5)*	9.6 (5.3-17.4)*
AST (U/L)	24.0 (18.0-27.0)	675.5 (345.0-1,386.0)*	406.2 (161.0-1,287.0)*	595.5 (394.0-1,214.5)*
ALT (U/L)	23.0 (17.3-28.0)	777.2 (253.7-1,531.7)*	769.5 (116.0-1,940.1)*	677.5 (368.7-1,728.8)*
CRNN (mg/dL)	0.6 (0.5-0.7)	0.7 (0.5-0.8)	0.8 (0.6-1.0)	0.7 (0.6-0.9)
PT-INR	0.99 (0.98-1.03)	1.8 (1.7-2.1)*	2.3 (1.9-3.2)*†	2.0 (1.7-2.3)*
HGF (ng/mL)	0.19 (0.14-0.29)	1.2 (0.8-1.5)*	2.4 (1.8-4.6)*†	1.4 (1.0-2.0)*
Plt ($\times 10^4/mm^3$)	20.8 (19.8-22.6)	14.3 (9.5-17.7)*	10.9 (8.3-14.8)*	12.1 (9.4-16.8)*
Coma grade ≥ II (%)		2/32 (6.3%)	14/18 (77.8%)†	16/50 (32.0%)
CTLV/SLV ratio		0.9 (0.8-1.2)	0.8 (0.7-0.9)‡	0.9 (0.8-1.1)
MELD score		19.0 (15.7-23.0)	26.0 (22.5-29.3)†	22.0 (17.2-25.7)
KCHC met (%)		3/32 (9.4)	10/18 (55.6)†	13/50 (26.0)
HE-prediction model		39.6 (21.3-49.9)	66.9 (53.0-76.4)†	48.6 (28.3-66.7)
JSS for ALF (1/2/3/4/5/6/7)		5/16/9/2/0/0/0	0/0/7/4/5/1/1	5/16/16/6/5/1/1

Note: The values represent the mean (range), median (25th–75th percentile), or number of patients.

*P < 0.01 (compared with control).

†P < 0.01 (compared with survivors).

‡P < 0.05 (compared with survivors).

Abbreviations: AIH, autoimmune hepatitis; ALT, alanine aminotransferase; AST, aspartate aminotransferase; CRNN, creatinine; HAV, hepatitis A virus; HBV, hepatitis B virus; Plt, platelet; T.Bil, total bilirubin.

TABLE 2. TIC and FFT Parameters in Control, Survivors, and Nonsurvivors

Parameters	Control		Survivors		Nonsurvivors		P Value
TTP (HA)	8.60	(7.55-11.15)	6.19	(4.93-7.85)‡	4.84	(3.21-6.12)‡	0.035†
TTP (PV)	19.80	(19.50-19.95)	9.62	(7.45-11.28)‡	8.15	(7.35-11.45)‡	0.731
TTP (LP)	20.00	(19.95-20.00)	13.10	(10.91-17.69)‡	7.80	(6.57-9.39)‡	0.005†
PI (HA)	119.32	(115.96-129.63)	117.43	(115.21-125.53)	115.63	(110.24-129.25)	0.333
PI (PV)	111.87	(109.67-121.01)	108.81	(104.24-132.75)	90.53	(65.98-112.27)‡	0.012†
PI (LP)	89.40	(82.61-95.69)	86.12	(79.75-101.23)	70.83	(53.76-105.53)*	0.026†
TI (HA, PV)	10.90	(8.80-12.15)	5.45	(3.59-7.52)‡	6.47	(4.84-7.96)‡	0.728
TI (HA, LP)	10.80	(8.65-12.20)	8.32	(7.20-10.12)‡	5.43	(3.73-6.15)‡	<0.0001†
TI (PV, LP)	0.40	(0.10-0.60)	4.16	(1.60-6.66)‡	1.45	(0.76-1.98)‡	0.056
HA-HVTT	8.28	(7.12-10.68)	1.85	(1.05-2.28)‡	1.75	(1.23-2.00)‡	0.445
Vmax (HA)	40.0	(35.0-41.0)	79.0	(59.0-89.0)‡	86.0	(62.8-97.7)‡	0.346
Vmax (PV)	21.0	(19.0-22.0)	15.7	(12.2-20.1)‡	13.0	(6.7-16.5)‡	0.205
HARI	0.66	(0.59-0.72)	0.75	(0.67-0.80)‡	0.81	(0.75-0.83)‡	0.148

Note: The values represent the median (25th-75th percentile).
*$P < 0.05$ (compared with control).
†There was a statistically significant difference between non-survivors and survivors.
‡$P < 0.01$ (compared with control).

PERFORMANCE CHARACTERISTICS OF TI (HA, LP) AND OTHER SCORING MODELS FOR PREDICTING POOR PROGNOSIS

The AUROC for the early prediction of poor prognosis was 0.953, 0.914, 0.861, 0.816, 0.731 for TI (HA, LP), JSS for ALF, HE-prediction model, MELD score, and KCHC, respectively (Table 4 and Supporting Fig. S2). The differences between TI (HA, LP) and the JSS for ALF or the HE-prediction model did not reach statistical significance ($P = 0.373$ and $P = 0.119$, respectively). In contrast, the differences between TI (HA, LP) and the MELD score or the KCHC were statistically significant ($P = 0.033$ and $P = 0.001$, respectively). The most appropriate cutoff value of TI (HA, LP) in predicting poor prognosis was 6.897 seconds, and the sensitivity, specificity, PPV, and NPV were 94.4%, 90.6%, 85.0%, and 96.7%, respectively.

SERIAL CHANGES IN TI (HA, LP) OF THE SURVIVORS AND NONSURVIVORS

Figure 4 shows the serial changes in TI (HA, LP) and the amount of change ΔTI (HA, LP) in 40 cases (28 survivors and 12 nonsurvivors) after 7 days.
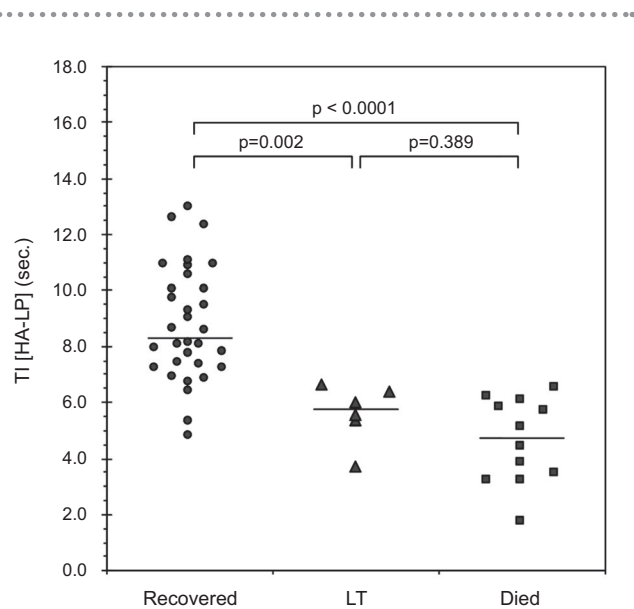

FIG. 3. TI (HA, LP) for all of the patients in each of the three categories: patients recovered with intensive therapies, including artificial liver support (recovered, n = 32 [8.31 (7.27-10.12)]; survived with LT, n = 6 [5.77 (5.38-6.29)]) and died without LT (died, n = 12 [4.73 (3.35-5.85)]). There were significant differences between patients who "recovered" versus "LT" ($P < 0.0001$), and "recovered" versus "those who died without LT" ($P = 0.002$), but not between "LT" and "those who died" ($P = 0.389$).

The causes of failure following CEUS were recovery (n = 4), LT (n = 2), death (n = 4), and deterioration of the general condition (n = 2). In the survivors, the

TABLE 3. Predictive Factors Associated With Nonsurvivors by Univariate and Multivariate Regression Models

Parameter	Univariate Analysis			Multivariate Analysis		
	OR (95% CI)		P Value	OR (95% CI)		P Value
Sex (male)	1.169	(0.363-3.756)	0.793			
Age	0.995	(0.959-1.041)	0.982			
Etiology (viral/others)*	3.571	(1.025-12.434)	0.045	8.785	(0.820-94.071)	0.172
T.Bil	1.041	(0.973-1.113)	0.239			
AST	0.985	(0.999-1.212)	0.804			
ALT	1.022	(0.983-1.002)	0.493			
CRNN	3.507	(0.707-28.071)	0.111			
PT-INR*	4.715	(1.283-17.322)	0.019	0.918	(0.122-6.206)	0.579
HGF*	5.120	(1.412-6.983)	0.005	2.216	(0.873-5.623)	0.094
Plt	0.899	(0.794-1.078)	0.092			
Coma grade ≥ II (present/absent)*	22.552	(8.574-321.457)	0.019	3.933	(0.032-51.056)	0.895
CTLV/SLV ratio*	0.099	(0.022-0.894)	0.014	0.129	(0.052-1.516)	0.135
TI (HA, LP)†	0.183	(0.062-0.532)	0.002	1.354	(1.036-1.769)	0.016

*Significant factor by univariate analysis.
†Significant factor by both univariate and multivariate analyses.
Abbreviations: ALT, alanine aminotransferase; AST, aspartate aminotransferase; CRNN, creatinine; Plt, platelet; T.Bil, total bilirubin.
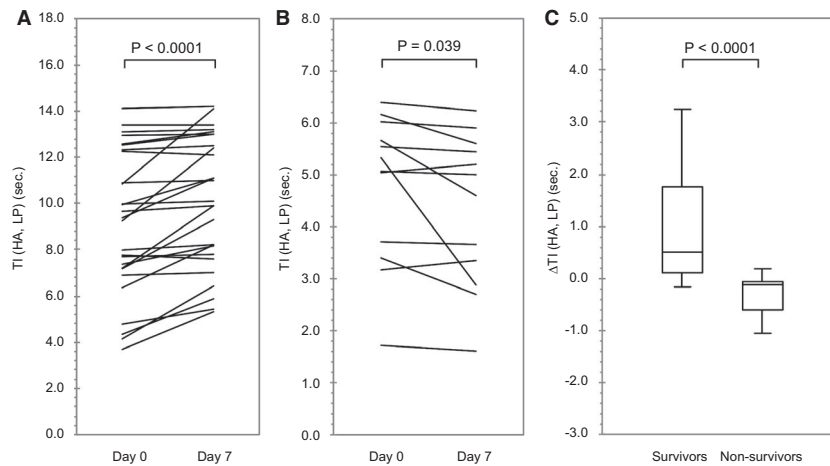

FIG. 4. Serial changes in the TI (HA, LP) of survivors (A), nonsurvivors (B), and ΔTI (HA, LP) (C). In survivors, the median TI (HA, LP) extended from 9.35 (7.17, 12.27) seconds to 10.01 (8.07, 12.62) seconds on day 7 ($P < 0.0001$). In contrast, in nonsurvivors, it was reduced from 5.19 (3.63, 5.75) seconds to 4.80 (3.23-5.48) seconds. The ΔTI (HA, LP) was +0.51 (0.12, 1.75) in survivors and –0.12 (–0.59, –0.06) in nonsurvivors.

median TI (HA, LP) extended from 9.35 seconds (7.17, 12.27) to 10.01 seconds (8.07, 12.62) on day 7 ($P < 0.0001$). In contrast, in nonsurvivors, it was reduced from 5.19 seconds (3.63, 5.75) to 4.80 seconds (3.23-5.48) on day 7 ($P = 0.039$). The ΔTI (HA, LP) was +0.51 (0.12, 1.75) in survivors and –0.12 (–0.59, –0.06) in nonsurvivors, with a significant difference between the two groups ($P < 0.0001$).

Discussion

In this prospective study, we evaluated 50 patients with ALF, measured the hepatic perfusion using CEUS with TIC analysis, and investigated its utility as a prognostic indicator. The results of the study confirm that in patients with ALF and massive hepatic necrosis, peculiar changes are seen on CEUS-based

TABLE 4. Diagnostic Accuracy of TI (HA, LP) and Other Scoring Models for the Prognostic Prediction

	TI (HA, LP)	JSS for ALF	HE-Prediction Model	MELD Score	KCHC
AUROC (95% CI)	0.953[*,†]	0.914[*]	0.861[‡]	0.816	0.731
	(0.895-0.998)	(0.849-0.979)	(0.757-0.965)	(0.693-0.939)	(0.602-0.860)
Cutoff value	6.897	3.0	48.9	20.0	Any 3 CPIs
Sensitivity	0.944	0.667	0.889	0.833	0.556
	(0.713-0.997)	(0.435-0.837)	(0.657-0.979)	(0.598-0.948)	(0.337-0.754)
Specificity	0.906	0.938	0.750	0.563	0.906
	(0.748-0.974)	(0.786-0.992)	(0.576-0.869)	(0.335-0.699)	(0.704-0.974)
PPV	0.850	0.846	0.667	0.517	0.769
	(0.707-1.000)	(0.674-1.000)	(0.478-0.855)	(0.332-0.768)	(0.540-0.998)
NPV	0.967	0.811	0.923	0.857	0.784
	(0.902-1.000)	(0.712-0.955)	(0.821-1.000)	(0.699-0.997)	(0.651-0.916)

[*]$P < 0.01$ (compared with KCHC).
[†]$P < 0.05$ (compared with MELD score).
[‡]$P < 0.05$ (compared with KCHC).
Abbreviations: AUROC, area under receiver the operating curve; CPI, clinical prognostic indicator.

hepatic perfusion. Moreover, TI (HA, LP), a real-time, noninvasive prognostic indicator, reveals tissue damage in these patients. These results show the potential of CEUS for making early predictions of the prognosis of patients with ALF and massive hepatic necrosis.

Sinusoids are low-pressure vascular channels that receive the HA and PV at the periphery of the lobules and deliver them into the central veins. Microbubble ultrasound contrast agents, such as Sonazoid, possess hemodynamic characteristics similar to those of the red blood cells and can reach the microvascular organs, allowing images to be captured. The changes observed in the hemodynamics of these organs lead to an understanding of the organ function.[23] The hepatic microcirculatory milieu, composed primarily of liver sinusoidal endothelial cells, hepatic stellate cells, and hepatic macrophages, have an essential role in liver homeostasis, including the preservation of the hepatocyte function and in control of inflammation.[31]

In our study, the Vmax (HA) in patients with ALF was significantly increased compared with that in controls. Moreover, the TTP (HA) in patients with ALF was significantly shorter than that in controls. Several previous reports using dynamic CT or Doppler ultrasound have shown similar results of increased HA blood flow during the acute phase in patients with ALF.[20,22] In contrast, TI (HA, LP) was statistically significantly shortened in nonsurvivors compared with that in controls and survivors. We concluded that the shortened TI (HA, LP) may have been caused by a

hepatic microcirculation disorder and the subsequent changes in the hepatic blood flow with reference to changes in blood flow in ALF and ALI (Supporting Fig. S3). In ALF, hypercytokinemia[32-34] and endotoxemia[35,36] are caused by severe inflammation and apoptosis. As a result, hypercoagulopathy occurs in the hepatic sinusoids and induces hepatic microcirculation disorders, such as an increase in sinusoidal pressure and a decrease in sinusoidal blood flow.[36-38] Hepatic microcirculation disorders and destruction of the sinusoidal structure due to massive hepatic necrosis may decrease the low-pressure portal venous blood flow. Moreover, fibrin deposition occurs in the hepatic sinusoids when Kupffer cells or hepatic macrophages are activated to increase the activity of the tissue factor, which is an initiator of the blood coagulation cascade.[39] Consequently, the slow transit rate of blood in the hepatic sinusoids, expanded interstitial space, and changes in the diffusion rate between the interstitial space and vascular space may result in peculiar changes in the hepatic perfusion.[21,40] On the other hand, as observed, the increased hepatic arterial blood flow is due to an inflammatory response,[41] hepatic arterial buffer response,[42,43] or destruction of the peribiliary capillary plexus.[44] Our study demonstrates that in ALF, when an increase in the sinusoidal pressure decreases the portal venous blood flow, the reduction in the hepatic parenchymal perfusion was immediately counterbalanced by the HA. Limited reports have focused on blood flow changes in ALF and ALI. Tanaka et al. showed that the Vmax of the

HA in acute hepatitis was significantly greater than that in controls.[22] Miyazaki et al. reported that in patients with ALI, the arrival time of HV was similar to that of PV and indicated the formation of intrahepatic shunts as a result of hepatic microcirculatory disturbances.[24] Feng et al. showed, in a rat model of acute radiation-induced liver injury, that HA-HVTT was shorter in the severe liver injury group than in the mild and moderate groups.[29] Adrian et al. reported that the HVTT decreased with the development of hepatic fibrosis, and it may be useful for the assessment of liver disease.[45,46] In this study, ALF significantly increased Vmax and HARI in the HA compared with those in controls. In the acute phase of ALF, massive necrosis, inflammation, and the expansion of extracellular matrix and fibrosis increase the elasticity of liver tissue, as measured using ultrasound elastography.[47,48] We speculated that the increase in HARI is due to the pressure of tissue on the bloodstream. In our study, it was confirmed that HA-HVTT in ALF was shorter than that in controls. However, HA-HVTT and some FFT parameters showed no statistically significant differences between survivors and nonsurvivors. The possible reason for this result is that HA-HVTT and some FFT parameters reveal the measurements in the hepatic in–out flow, and indirectly infer the degree of the hepatic microcirculation, whereas TI (HA, LP) is a parameter that more directly reflects the hepatic microcirculation disorder. Therefore, TI (HA, LP), as a sensitive indicator of both massive hepatic necrosis and the hepatic microcirculation disorder, is important in early diagnosis of ALF with poor prognosis.

We also observed that TI (HA, LP) showed the highest AUROC compared with the existing prognostic models for ALF, such as the JSS for ALF, the HE-prediction model, the MELD score, and the KCHC. Remarkably, TI (HA, LP) shows statistically superior results to the MELD score and the KCHC, which are used commonly worldwide. Moreover, it must be considered that CEUS is a minimally invasive technique that can be repeated easily. Thus, TI (HA, LP) may be used as an early, noninvasive predictor for the prognosis for ALF in evaluating the need for LT. In our study, the serial changes in TI (HA, LP) and the amount of change, ΔTI (HA, LP), were observed after 7 days. In the survivors, the median TI (HA, LP) was significantly higher, and it was significantly lower in nonsurvivors. Significant differences in ΔTI (HA, LP) were noted between the two groups.

The evaluation of hepatic perfusion by CEUS is a simple and noninvasive test that can be performed in real time and is repeatable. Continuous TI (HA, LP) measurements may complement the assessment of the baseline value and may also be a useful parameter to reflect the need for LT, because the medical condition of patients with ALF can change rapidly.

This study has several limitations. First, the sample size is small. Larger-scale prospective clinical studies are needed to confirm these findings. Second, compared with dynamic CT, which is used commonly, CEUS is an operator-dependent examination. CEUS evaluates only a single scanning plane, which prevents us from understanding the global image of ALF. CEUS and TIC analysis applications are not available on all ultrasound instruments. Moreover, the results of our study obtained using the Aplio500 ultrasound scanner with Sonazoid may not translate directly to those obtained with other ultrasound machines and other microbubble ultrasound contrast agents. Third, acetaminophen overdose is the leading cause of ALF in the developed world; however, there was only 1 patient in this study with acetaminophen as the etiology of ALF. Finally, the influence of selection bias cannot be denied.

In conclusion, the findings of this study suggest that TI (HA, LP) measured by CEUS with TIC analysis reflects the severity of liver damage in patients with ALF. It may be used as an early, precise prognostic biomarker for ALF, making it useful in clinical decision making.

REFERENCES

1) Trey C, Davidson CS. The management of fulminant hepatic failure. Prog Liver Dis 1970;3:282-298.
2) Wendon J, Cordoba J, Dhawan A, Larsen FS, Manns M, Nevens F, et al. EASL Clinical Practical Guidelines on the management of acute (fulminant) liver failure. J Hepatol 2017;66:1047-1081.

3) Takikawa Y, Suzuki K. Clinical epidemiology of fulminant hepatitis in Japan. Hepatol Res 2008;38(Suppl. 1):S14-S18.

4) Oketani M, Ido A, Nakayama N, Takikawa Y, Naiki T, Yamagishi Y, et al. Etiology and prognosis of fulminant hepatitis and late-onset hepatic failure in Japan: summary of the annual nationwide survey between 2004 and 2009. Hepatol Res 2013;43:97-105.

5) Bernal W, Hyyrylainen A, Gera A, Audimoolam VK, McPhail MJW, Auzinger G, et al. Lessons from look-back in acute liver failure? A single centre experience of 3300 patients. J Hepatol 2013;59:74-80.

6) Koch DG, Tillman H, Durkalski V, Lee WM, Reuben A. Development of a model to predict transplant-free survival of patients with acute liver failure. Clin Gastroenterol Hepatol 2016;14:1199-1206.e1192.

7) Reuben A, Tillman H, Fontana RJ, Davern T, McGuire B, Stravitz RT, et al. Outcomes in adults with acute liver failure between 1998 and 2013: an observational cohort study. Ann Intern Med 2016;164:724-732.

8) Batra Y, Acharya SK. Acute liver failure: prognostic markers. Indian J Gastroenterol 2003;22(Suppl. 2):S66-S68.

9) Takikawa Y, Endo R, Suzuki K, Tsubouchi H. Early prediction of short-term development of hepatic encephalopathy in patients with acute liver disease unrelated to paracetamol. A prospective study in Japan. J Hepatol 2009;51:1021-1029.

10) Stravitz RT, Kramer AH, Davern T, Shaikh AOS, Caldwell SH, Mehta RL, et al. Intensive care of patients with acute liver failure: recommendations of the U.S. Acute Liver Failure Study Group. Crit Care Med 2007;35:2498-2508.

11) Williams R, Wendon J. Indications for orthotopic liver transplantation in fulminant liver failure. Hepatology 1994;20:S5-S10.

12) Rockey DC, Caldwell SH, Goodman ZD, Nelson RC, Smith AD. Liver biopsy. Hepatology 2009;49:1017-1044.

13) Kamath PS, Kim WR. The model for end-stage liver disease (MELD). Hepatology 2007;45:797-805.

14) O'Grady JG, Alexander GJ, Hayllar KM, Williams R. Early indicators of prognosis in fulminant hepatic failure. Gastroenterology 1989;97:439-445.

15) Naiki T, Nakayama N, Mochida S, Oketani M, Takikawa Y, Suzuki K, et al. Novel scoring system as a useful model to predict the outcome of patients with acute liver failure: application to indication criteria for liver transplantation. Hepatol Res 2012;42:68-75.

16) Cholongitas E, Germani G, Burroughs AK. Prioritization for liver transplantation. Nat Rev Gastroenterol Hepatol 2010;7:659-668.

17) Wanless IR, Wong F, Blendis LM, Greig P, Heathcote EJ, Levy G. Hepatic and portal vein thrombosis in cirrhosis: possible role in development of parenchymal extinction and portal hypertension. Hepatology 1995;21:1238-1247.

18) Wanless IR, Shiota K. The pathogenesis of nonalcoholic steatohepatitis and other fatty liver diseases: a four-step model including the role of lipid release and hepatic venular obstruction in the progression to cirrhosis. Semin Liver Dis 2004;24:99-106.

19) Murakami T, Baron RL, Peterson MS. Liver necrosis and regeneration after fulminant hepatitis: pathologic correlation with CT and MR findings. Radiology 1996;198:239-242.

20) He N, Zhao D, Chen F. MDCT dynamic enhancement appearances in acute liver failure. Radiol Infect Dis 2015;2:146-149.

21) Cakir B, Teksam M, Tarhan NC, Isiklar I, Tutar NU, Ozcay F, et al. Unusual MDCT and sonography findings in fulminant hepatic failure resulting from hepatitis A infection. Am J Roentgenol 2005;185:1033-1035.

22) Tanaka K, Mitsui K, Morimoto M, Numata K, Inoue S, Takamura Y, et al. Increased hepatic arterial blood flow in acute viral hepatitis: assessment by color Doppler sonography. Hepatology 1993;18:21-27.

23) Emanuel AL, Meijer RI, van Poelgeest E, Spoor P, Serne EH, Eringa EC. Contrast-enhanced ultrasound for quantification of tissue perfusion in humans. Microcirculation 2020;27:e12588.

24) Miyazaki M, Kato M, Tanaka M, Tanaka K, Takao S, Kohjima M, et al. Contrast-enhanced ultrasonography using Sonazoid to evaluate changes in hepatic hemodynamics in acute liver injury. J Gastroenterol Hepatol 2011;26:1749-1756.

25) Gauthier TP, Chebil M, Peronneau P, Lassau N. In vitro evaluation of the impact of ultrasound scanner settings and contrast bolus volume on time-intensity curves. Ultrasonics 2012;52:12-19.

26) Yeh CK, Yang MJ, Li PC. Contrast-specific ultrasonic flow measurements based on both input and output time intensities. Ultrasound Med Biol 2003;29:671-678.

27) Sugawara K, Nakayama N, Mochida S. Acute liver failure in Japan: definition, classification, and prediction of the outcome. J Gastroenterol 2012;47:849-861.

28) Claudon M, Dietrich CF, Choi BI, Cosgrove DO, Kudo M, Nolsøe CP, et al. Guidelines and good clinical practice recommendations for contrast enhanced ultrasound (CEUS) in the liver—update 2012: a WFUMB-EFSUMB initiative in cooperation with representatives of AFSUMB, AIUM, ASUM, FLAUS and ICUS. Ultrasound Med Biol 2013;39:187-210.

29) Feng J, Chen SB, Wu SJ, Sun P, Xin TY, Chen YZ. Quantitative analysis of contrast-enhanced ultrasonography in acute radiation-induced liver injury: an animal model. Exp Ther Med 2015;10:1807-1811.

30) Urata K, Kawasaki S, Matsunami H, Hashikura Y, Ikegami T, Ishizone S, et al. Calculation of child and adult standard liver volume for liver transplantation. Hepatology 1995;21:1317-1321.

31) Gracia-Sancho J, Marrone G, Fernandez-Iglesias A. Hepatic microcirculation and mechanisms of portal hypertension. Nat Rev Gastroenterol Hepatol 2019;16:221-234.

32) Guo L-M, Liu J-Y, Xu D-Z, Li B-S, Han H, Wang L-H, et al. Application of molecular adsorbents recirculating system to remove NO and cytokines in severe liver failure patients with multiple organ dysfunction syndrome. Liver Int 2003;23(Suppl. 3):16-20.

33) Sen S, Davies NA, Mookerjee RP, Cheshire LM, Hodges SJ, Williams R, et al. Pathophysiological effects of albumin dialysis in acute-on-chronic liver failure: a randomized controlled study. Liver Transpl 2004;10:1109-1119.

34) Lentsch AB, Yoshidome H, Cheadle WG, Miller FN, Edwards MJ. Chemokine involvement in hepatic ischemia/reperfusion injury in mice: roles for macrophage inflammatory protein-2 and Kupffer cells. Hepatology 1998;27:507-512.

35) Jaeschke H, Bajt ML. Critical role of CXC chemokines in endotoxemic liver injury in mice. J Leukoc Biol 2004;76:1089-1090; author reply 1091-1082.

36) Le Bail B, Bioulac-Sage P, Senuita R, Quinton A, Saric J, Balabaud C. Fine structure of hepatic sinusoids and sinusoidal cells in disease. J Electron Microsc Tech 1990;14:257-282.

37) Mochida S, Arai M, Ohno A, Yamanobe F, Ishikawa K, Matsui A, et al. Deranged blood coagulation equilibrium as a factor of massive liver necrosis following endotoxin administration in partially hepatectomized rats. Hepatology 1999;29:1532-1540.

38) Vollmar B, Menger MD. The hepatic microcirculation: mechanistic contributions and therapeutic targets in liver injury and repair. Physiol Rev 2009;89:1269-1339.

39) Tsutsui H, Nishiguchi S. Importance of Kupffer cells in the development of acute liver injuries in mice. Int J Mol Sci 2014;15:7711-7730.

40) Itai Y, Ohtomo K, Kokubo T, Minami M, Yoshida H. CT and MR imaging of postnecrotic liver scars. J Comput Assist Tomogr 1988;12:971-975.

41) Lang CH, Bagby GJ, Ferguson JL, Spitzer J. Cardiac output and redistribution of organ blood flow in hypermetabolic sepsis. Am J Physiol 1984;246(Pt 2):R331-R337.

42) Lautt WW. Mechanism and role of intrinsic regulation of hepatic arterial blood flow: hepatic arterial buffer response. Am J Physiol 1985;249:G549-G556.

43) Gulberg V, Haag K, Rossle M, Gerbes AL. Hepatic arterial buffer response in patients with advanced cirrhosis. HEPATOLOGY 2002;35:630-634.

44) Ekataksin W, Kaneda K. Liver microvascular architecture: an insight into the pathophysiology of portal hypertension. Semin Liver Dis 1999;19:359-382.

45) Lim AKP, Patel N, Eckersley RJ, Goldin RD, Thomas HC, Cosgrove DO, et al. Hepatic vein transit time of SonoVue: a comparative study with Levovist. Radiology 2006;240:130-135.

46) Lim AK, Taylor-Robinson SD, Patel N, Eckersley RJ, Goldin RD, Hamilton G, et al. Hepatic vein transit times using a microbubble agent can predict disease severity non-invasively in patients with hepatitis C. Gut 2005;54:128-133.

47) **Kuroda H**, **Kakisaka K**, Oikawa T, Onodera M, Miyamoto Y, Sawara K, et al. Liver stiffness measured by acoustic radiation force impulse elastography reflects the severity of liver damage and prognosis in patients with acute liver failure. Hepatol Res 2015;45:571-577.

48) Sagir A, Erhardt A, Schmitt M, Häussinger D. Transient elastography is unreliable for detection of cirrhosis in patients with acute liver damage. HEPATOLOGY 2008;47:592-595.

Author names in bold designate shared co-first authorship.

Supporting Information

Additional Supporting Information may be found at onlinelibrary.wiley.com/doi/10.1002/hep.31615/suppinfo.